Proceedings of the 2003 IEEE
International Conference on Robotics & Automation
Taipei, Taiwan, September 14-19, 2003

Passivity-Based High-Fidelity Haptic Rendering of Contact

Mohsen Mahvash and Vincent Hayward

Center For Intelligent Machines
McGill University, Montréal, Québec, H3A 2A7 Canada
mahvash|hayward@cim.mcgill.ca

Abstract

A method is described whereby the virtual haptic interaction with deformable elastic objects is created in terms of two processes: a slow process which carries out the simulation, and a fast process to render forces. Passivity theory is used to design an update strategy which reproduces exactly pre-computed responses between a tool and an object. This yields a design procedure for adjustable local models which guarantee the passivity of the interaction while preserving fidelity. Two examples of local models are given and some experimental results are reported.

1 Introduction

Creating a force reflecting virtual environment which simulates the details of actual contacts is a challenge. Moreover, the stability of an artificial haptic interaction is usually lost due to the discrete nature of the simulation, even when the update rate is in principle sufficiently high to represent the physics of a contact. We propose a method which provides stability as well as fidelity of the interaction in a multi-rate setting. A low rate process passes the contact responses to a fast control unit which provides passivity while preserving the details of the response. The computations done by the fast control unit are minimal, so this unit can be conveniently implemented using ordinary computing platforms or embedded processors.

The design of a passivity-based control strategy using model updates is first discussed in the general case. The technique is exemplified for the case of "poking" a surface and for the case of 3D interaction of a given tool with a virtual elastic object which can be inhomogeneous and/or anisotropic. The simulation also includes friction.

A useful approach to the stability of a haptic interaction is based on passivity because a system model of the operator is not required in the design. What is required instead is passivity of the artificial system which creates the virtual haptic interaction and that of the operator. Stability is achieved by providing passivity for all the components of the system. This is similar to what happens in the physical world when objects come into contact. Passivity and fidelity of the artificial system are sufficient to create realistic artificial contacts whether the interaction is stable or not.

2 Related Work

Anderson and Spong pioneered the use of passivity theory in teleoperation systems. They introduced the basic notions needed to analyze force feedback systems in terms of passivity [2]. A complete system was divided into four passive subsystems and a non-passive communication block. This made it possible to design a control such that the complete system remained passive. Niemeyer and Slotine adopted a similar framework and successfully used the notion of wave variables to provide stability as well as explicit design tradeoffs regarding fidelity [12]. This framework was also used by Yokokohji *et al.* to deal with fluctuating time delays [14].

Colgate and Shenkel used passivity to study the the effect of discrete time implementation of a virtual environment and derived a sufficient condition for stability [4]. Miller *et al.* later derived a sufficient condition for stability for a broad class of nonlinear and time delayed virtual environments [11]. To provide stability, the approach is to introduce a virtual coupling to combat the effects of delay and discretization [1, 3, 11]. Recently, Hannaford and Ryu employed a different strategy involving a passivity observer coupled to a time-varying passivity controller designed to inject damping into the system [5]. In all these approaches, fidelity may be compromised to gain stabillity.

The excellent survey by Salisbury *et al.* describes

many important issues in haptic rendering, including the need for fidelity in some applications [13]. The authors suggest that calculating forces from a potential field can provide passivity for contact interaction with three dimensional virtual bodies, but the design of these fields was left as an open question.

The present paper adopts notions developed for teleoperation and uses them for haptics, considering that the remote environment, the slave robot, and the communication link are replaced by the computational simulation of a tool interacting with a body. Thus, the five basic subsystems of teleoperation are replaced by three in haptics as seen next.

3 Passivity in Haptic Interaction Systems

Definition: A system with input v, output f and initial energy $E(0)$, $v(t), f(t) \in \mathbb{R}^n$ is passive if [8]:

$$\int_0^t f(\tau)^\top v(\tau)\, d\tau + E(0) \geq 0 \qquad (1)$$

for all functions v, f, and $t \geq 0$, see Figure 1.

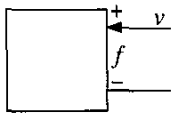

Figure 1: A block element.

A haptic interaction system is represented in block diagram format in the Figure 2.

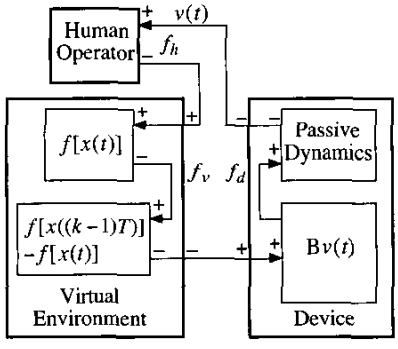

Figure 2: Haptic interaction system block diagram.

The complete system consists of three subsystems: the human operator, the virtual environment and the haptic device. No matter how well constructed, a device always has some residual damping. The device is thus represented by two sub-blocks: a damper $\mathbf{B}\, v$, where $\mathbf{B} > 0$, and a block which represents the other device dynamics which, excluding the force transducing element, are passive. The virtual environment is represented by two sub-blocks: $f[x(t)]$, the continuous time realization of a virtual environment and $f[x((k-1)T)] - f[x(t)]$, the difference between the discrete and the continuous time realizations of the same environment.

The damper sub-block and the block which represents the effect of delay and discretization can be lumped into one subsystem as in Figure 3. If the continuous realization of the virtual environment is passive, since the device dynamics are passive, the haptic interaction will be passive if the subsystem of Figure 3 is also passive.

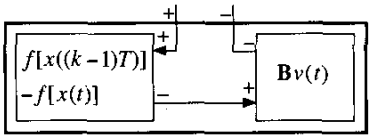

Figure 3: Subsystem of the complete system of Fig.2.

The subsystem of Figure 3 will be passive, if

$$2T\,[f(x_1) - f(x_2)]^\top (x_1 - x_2) < (x_1 - x_2)^\top \mathbf{B}\,(x_1 - x_2), \quad \forall x_1, x_2 \in \mathbb{R}^3. \qquad (2)$$

Substituting x_1 by $x(\tau)$, x_2 by $x((k-1)T)$, and $(x_1 - x_2)$ by $[\tau - (k-1)T]v(\tau)$, for small T, Eq. (2) yields:

$$\frac{2T}{\tau - (k-1)T}\,[f(x(\tau)) - f(x((k-1)T))]^\top v(\tau) < v(\tau)^\top \mathbf{B}\, v(\tau). \qquad (3)$$

Then, for $(k+1)T \geq \tau \geq kT$:

$$[f(x(\tau)) - f(x((k-1)T))]^\top v(\tau) < v(\tau)^\top \mathbf{B}\, v(\tau) \qquad (4)$$

Integrating both sides of Eq. (4) gives:

$$\int_0^t [f(x(\tau)) - f(x((k-1)T))]^\top v(\tau)\, d\tau < \int_0^t v(\tau)^\top \mathbf{B}\, v(\tau)\, d\tau, \qquad (5)$$

that is

$$\int_0^t \left[f(x((k-1)T)) - f(x(\tau)) + \mathbf{B}\, v(\tau)\right]^\top v(\tau)\, d\tau > 0. \qquad (6)$$

Eq. 6 is the passivity condition for the subsystem of Fig. 3 for $E(0) = 0$. For x_1 close to x_2:

$$[f(x_1) - f(x_2)]^\top \approx \mathbf{J}_f(x_1 - x_2), \tag{7}$$

Cond. (2) can be simplified to:

$$\mathbf{B} > 2T\,\mathbf{J}_f(x) \tag{8}$$

Cond. (2) or Cond. (8) mean that the passivity of the haptic interaction, as seen from the end-effector of a device, for a passive virtual environment $f(x)$ can be achieved by a sufficiently high rate force update and without the need for virtual coupling.

4 Passive Model Update

We show that $f(x)$ can be passively re-created in terms of force updating models running at high-rate but updated at low rate by a slow process, see Fig. 4. Let i be the time slot used by the low rate process from time t_i to t_{i+1} and let $f_i(x)$ be the local model during that time slot:

$$f(x) = f_i(x), \quad t_i \le t < t_{i+1} \tag{9}$$

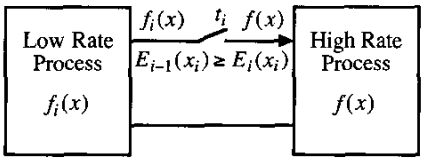

Figure 4: Multi rate haptic rendering.

The $f_i(x)$'s are conservative passive models which locally fits the contact simulation responses calculated by the low rate process.

The passivity condition for $f(x(t))$ is:

$$E(t) = \int_0^t f(x(\tau))^\top v(\tau)\,d\tau \ge 0 \tag{10}$$

$E(t)$ can be written in terms of f_i:

$$E(t) = \sum_{i=0}^{n-1}\left(\int_{t_i}^{t_{i+1}} f_i(x(\tau))^\top v(\tau)\,d\tau\right) + \int_{t_n}^{t} f_i(x(\tau))^\top v(\tau)\,d\tau. \tag{11}$$

For $f_i(x)$ conservative, $\nabla \times f_i = 0$,

$$\int_{t_i}^{t_{i+1}} f(x(\tau))^\top v(\tau)\,d\tau = \tag{12}$$

$$\int_{t_i}^{t_{i+1}} f(x(\tau))^\top \frac{dx(\tau)}{d\tau}d\tau = \int_C f(x)^\top dx \tag{13}$$

$$= \int_{x_i}^{x_{i+1}} f(y)^\top dy = E_i(x_{i+1}) - E_i(x_i), \tag{14}$$

where $x_i = x(t_i)$ and where $E_i(x)$ is defined by

$$E_i(x) = \int_{x_0}^{x} f_i(y)^\top dy. \tag{15}$$

Using Eq. (14), Eq (11) can be written:

$$\begin{aligned} E(t) &= \sum_{i=0}^{n-1}[E_i(x_{i+1}) - E_i(x_i)] + E_n(x) - E_n(x_n) \\ &= \sum_{i=1}^{n} E_{i-1}(x_i) - \sum_{i=0}^{n-1} E_i(x_i) - E_n(x_n) + E_n(x) \\ &= \sum_{i=1}^{n}[E_{i-1}(x_i) - E_i(x_i)] + E_n(x). \end{aligned} \tag{16}$$

Suppose now that f_i is adjusted at time t_i such that

$$E_{i-1}(x_i) \ge E_i(x_i), \tag{17}$$

then

$$E(t) \ge E_n(x) \ge 0, \tag{18}$$

therefore f is passive.

Several strategies can be used to insure that Cond. (17) is met. In the next Section, two examples are discussed.

5 Passive Rendering Examples

The first example shows how poking a virtual surface with a virtual tool can be rendered with high fidelity. The second shows how the theory can be applied to the case of interaction with deformable bodies. The two examples used different passive update strategies.

5.1 Local Linear Impedances And Adjusted Relaxed States

5.1.1 Strategy

The local models are selected (among other possibilities) to be linear impedances that locally fit single valued simulation responses. Such linear impedances are associated with an energy which is easily evaluated and which depends on three quantities: a state, the value of the state for which the energy is zero, i.e., the "relaxed state", and the impedance itself. The relaxed states are adjusted to preserve the energy condition Cond. (17).

For interactions along the poking dimension, linear local models are given by:

$$f_i(x) = \begin{cases} 0 & x \leq c_i, \\ k_i(x - c_i) & x > c_i, \end{cases} \quad (19)$$

where the c_i are the relaxed states and the k_i are the impedances locally fitting the output force of the low rate process. The value of k_i can be expressed in terms of the desired output force f_i at time t_i:

$$k_i = \frac{f_{i-1} - f_i}{x_{i-1} - x_i}. \quad (20)$$

$E_i(x)$ for f_i is given by

$$E_i(x) = \frac{1}{2} k_i (x - c_i)^2. \quad (21)$$

The equality of Cond. (17) is used to find an energy response equal to the desired response:

$$\frac{1}{2} k_{i-1}(x_i - c_{i-1})^2 = \frac{1}{2} k_i (x_i - c_i)^2. \quad (22)$$

Solving for c_i gives a value that guarantees a passive update:

$$c_i = (1 - \sqrt{\frac{k_{i-1}}{k_i}}) x_i + \sqrt{\frac{k_{i-1}}{k_i}} c_{i-1}. \quad (23)$$

When $k_i = 0$, i.e. moving in free space, k_i and c_i are updated by:

$$\begin{aligned} k_i = 0,\ c_i = x, & \quad \text{if } E_{i-1} = 0, \\ k_i = k_{i-1},\ c_i = c_{i-1}, & \quad \text{if } E_{i-1} > 0. \end{aligned} \quad (24)$$

5.1.2 One Dimensional Interaction With Nonlinear Response

The strategy of last section was implemented to evaluate the gain in stability performance in comparison with other strategies.

The forces were generated by a PenCat/Pro™ haptic device (Immersion Canada Inc.). This device was powered by Lorenz flat-coil actuators driving the end-effector in a single stage via a planar linkage. These actuators were in turn powered by current amplifiers. As a result, the device had very little damping and friction, a best case for fidelity, but a worse case for inherent stability margin in the sense discussed in Section 3.

The simulation program consisted of two independent real-time threads running under RTLinux-3. One thread provided for rendering the forces and the other for computing the contact simulation. Here, the virtual environment is a nonlinear wall with k measured in N/m and x in m.

$$f(x) = \begin{cases} 0 & 0 \leq x \\ 100\,k\,x^2 & 0 < x \leq 0.005 \\ k(x - 0.000025) & 0.005 < x \end{cases} \quad (25)$$

The response parameters are chosen such that k alone defines an appropriate stability margin as defined by Cond. 8. To see that, consider that inside the quadratic portion of the response when $x \leq 0.005$, $\mathbf{J}_f$ reduces to $200\,k\,x$ and therefore is bounded by k. Thus, the same margin applies to the two portions of the response.

In order to create repeatable experimental conditions, the handle of the device was loaded by a rubber band stretched to create an equilibrium around 1 N. Then, k was increase until small disturbances determined the onset of limit-cycles. This was tested for three different methods:

1. A single process at various rates.
2. Two processes. The first one computed a response as in Eq. (25) at various rates as above, and a second rendered forces at a rate of 2,000 Hz using linear interpolation from one update to the next.
3. Two processes as described in the last section. The first one was the same as above, and the second one also ran at 2,000 Hz but implemented the passive updates strategy.

The results listed in Table 1 show the largest impedance values which could be rendered in a stable fashion for all conditions.

The results indicate that the linear interpolation method performs better than the single update method. The passive update method, however, gave a constant stability margin even when the update rate decreased from 2,000 to 100 Hz. The results also show that the passivity based approach strategy could realize larger impedances than the other methods.

Rate (Hz)	Single thread k (N/m)	Linear interpolation k (N/m)	Passive update k (N/m)
2000	170	170	212
1000	120	160	212
500	93	127	212
250	63	110	212
200	57	104	212
100	38	85	212

Table 1: Achievable impedances for three strategies.

5.2 Deformable Body With Nonlinear Response

The same strategy can be extended to the three dimensional haptic rendering of deformable bodies. It could be applied in settings which use FEM, BEM, or LEM methods for the simulation of deformation, provided that a low rate process provides local impedances to a high rate process (*e.g.* [7]). The development of a passive update technique for these cases is possible but is outside the scope of this paper. On the other hand, methods based on pre-calculated responses, as described in [9, 10], are simple enough to be treated in this section.

5.2.1 Pre-Calculated Response of a Deformable Body

A deformable body at rest is represented by a free-form surface meshed into triangular elements. The interaction of a tool with the body is encoded as a finite set of normal force-deflection responses stored for each node (penetration in a direction normal to the undeformed surface with a given tool). Each deflection maps to a force that has a magnitude and a direction. An assumption that we make is that the force direction is assumed to remain invariant with deflection (if needed, a dependency could be included), therefore, each of these responses requires the specification of a vector and of a single-valued function $f_i(\delta)$. This is depicted by Figure 5a. During interaction, a point of contact x_c is known on the flat surface of the patch. A vector u_n, termed the *response normal vector*, is defined by:

$$u_n = \sum_{j=1,2,3} n_i^j(x_c)\ u_i^j, \tag{26}$$

where the u_i^j are the unit deflection normal vectors of the responses at node j of the element i, and where n_i^j is an interpolation function for element i for each node j which depends on x_c. A common choice in continuous mechanics that we use here is based on natural coordinates:

$$n_i^j(x) = \frac{A_j(x)}{A^i} \tag{27}$$

where A^i is the area of the element i and A_j is the area of the triangle formed by the contact point and two nodes as defined in Figure 5b. A key property of the interpolation approach is to ensure continuity of the normal response vector over the surface of the body. This vector is almost always different from the geometrical normal vector defined by the patch.

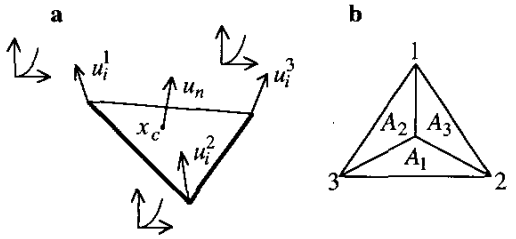

Figure 5: For each triangular element i, the vertices are associated to a normal $u_i^j, j = 1, 2, 3$ and to a response along this normal (**a**). A point inside a triangle defines three areas labeled as indicated (**b**).

5.2.2 Slow Simulating Process And Fast Rendering Process

The role of the low rate simulation process is to supply the vertices locations, the deflection normals at these vertices, and the force deflection curves of one element at a time. The active element, i.e. the element in contact with the tool, is determined using an interference detection method similar to the god object approach in haptics [15]. Since the elements are large relatively to a typical tool speed, this can be done at low rate; 100 Hz is sufficient (moving at 1 m/s over 10 mm patches).

The interaction force, however, is evaluated at high rate. The normal component is interpolated from three pre-calculated force-deflection responses, each representing the response of an *actual* contact (not an approximation) of a given body interacting with a given tool:

$$f_{in}(x) = \sum_{j=1,2,3} n_i^j(x_c)\ f_i^j(\delta_n(x_c)) \tag{28}$$

An element switch is allowed when the contact point x_c crosses the edges of the active element. If available, a new element is accepted and the point x_c moved to it. This is accomplished with dual-threaded code communicating by a first-in-first-out (FIFO) queue. Two cases can arise: if x_c belongs to a neighboring patch found in the FIFO, a new element is accepted, otherwise the rendering process carries on with same patch. This gives a correct response at a wrong place, but there is no loss of continuity nor of passivity even if there is loss of synchronization between the movement of the tool and the simulation process.

We now add friction to the local model. Inside element i:

$$f_i(x) = f_{in}(x)u_n + f_{it}(x)u_t \tag{29}$$

The contact point x_c is a function of the measured virtual tool position x set by the user. We first look at the case when there is no sliding, that is, when x_c is invariant. Referring to Figure 6, the deflection δ at the point of contact is given by:

$$\delta = x - x_c = \delta_n u_n + \delta_t u_t, \tag{30}$$

where δ_n and δ_t are the components of δ in a local frame. The penetration is defined by δ_n. The component δ_t may be viewed as presliding displacement in friction modeling [6].[1] When there is no sliding, $\delta_t < \delta_L$, where δ_L is the displacement under which there is no sliding.

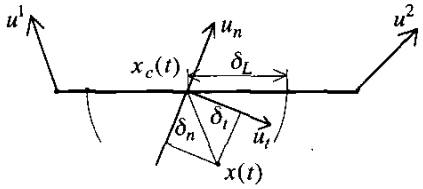

Figure 6: For clarity, only the two-dimensional case is illustrated. The extension to three dimensions is straightforward. u_n is defined in terms of u^1 and u^2. This defines a frame with origin at the point of contact x_c. When δ_t reaches δ_L, sliding occurs.

The pre-displacement δ_t is simply mapped onto the patch surface to determine the movements of x_c such that δ_t never exceeds δ_L [6]. The friction force at the sliding limit is $f_{i_t}(x) = \mu f_{i_n}(x)$ where μ is the limiting friction coefficient. Coulomb's law is invoked to assume that the friction force is independent from the area of contact.

5.2.3 Passivity

When poking without sliding, point x_c is created by projecting the x onto the surface of the active element, but only when x is outside the previous active element. From the time of creation of point x_C until the next creation, δ is replaced by $\delta - \delta_0$ where δ_0 is the initial value of δ. This adjustment of the relaxed state ensures that Cond (17) is satisfied.

During sliding, x_c moves within the element surface. If the energy lost due to sliding friction is greater than the change of $E_i(x)$ due to the sliding movement of contact point, the energy $E(t)$ of the interaction must be greater than $E_i(x)$, so passivity is preserved. During element switch, since the change in force is continuous, even with updates at low rate, Cond. (17) is satisfied which eliminates the need for further adjustment of the local model.

[1] In [9], it is verified that δ_t is largely independent from δ_n for rubbery materials. It is probably also the case for many biomaterials.

5.2.4 Implementation

The model was tested with a deformable cylindrical virtual body. The normal responses were:

$$f(\delta_n) = \begin{cases} 0 & 0 \leq \delta_n \\ 100\ k{\delta_n}^2 & 0 < \delta_n \leq 0.005 \\ k(\delta_n - 0.000025) & 0.005 < \delta_n \end{cases} \tag{31}$$

In this model, the system returns the nonlinear response at high rate and performs simulation at low rate. Figure 7 shows the user interface used in the test. The low rate process was running at only 100 Hz, yet the simulation was stable for $k_{max} = 170$ N/m for the fast process running at 2,000 Hz, as found in the experiment described in the previous section.

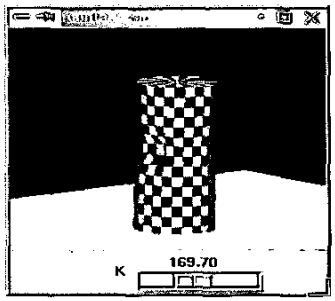

Figure 7: Tool contact simulation.

5.3 Conclusion

It was shown that low-rate yet stable haptic simulations involving tools interacting with deformable bodies could be achieved without compromising fidelity. In particular, various tool shapes and anisotropic and/or in-homogenous body can be haptically represented using a pre-calculated force-deflection response approach. This was achieved using a dual-threaded system having a slow thread executing the simulation itself and a high rate thread locally rendering the interaction. Passivity theory was used to constructively design two different local update strategies that guaranteed passivity under a wide range of circumstances.

Work is under way to extend the same framework to multiple contacts, and to tool movements with six degrees of freedom. It should also be extended to time varying dissipative virtual environments involving viscosity, plasticity, cutting and other forms of damage insofar as the application requires the simulation of these phenomena.

Acknowledgements

This research was funded by the project "Reality-based Modeling and Simulation of Physical Systems in Virtual Environments" of IRIS, the Institute for Robotics and Intelligent Systems (Canada's Network of Centers of Excellence). Additional funding is provided by NSERC, the Natural Sciences and Engineering Council of Canada, in the form of an operating grant for the second author.

References

[1] Adams, R. J., and Hannaford, B. 1999. Stable Haptic Interaction With Virtual Environments. *IEEE T. Robot. Automat.* 15:465–474.

[2] Anderson, R. J. and Spong., M. 1989. Bilateral Control of Teleoperators with Time Delay. *IEEE T. on Aut. Control.* 34(5):494–501.

[3] Brown, J. M, and Colgate, J. E. 1997. Passive Implementation of Multi- body Simulations for Haptic Display. Proc. *International Mechanical Engineering Congress and Exhibition,* Vol. 61, pp.85–92.

[4] Colgate, J. E., and Schenkel, G.G. 1997. Passivity of a Class of Sampled-Data Systems: Application to Haptic Interfaces. *J. of Robotic Systems.* 14(1):37-47.

[5] Hannaford, B., Ryu, J.-H. 2002. Stable Haptic Interaction with Virtual Environments. *IEEE T. Robot. and Automat.*, 18(1).

[6] Hayward, V., Armstrong, B., 2000. A New Computational Model of Friction Applied to Haptic Rendering. In *Experimental Robotics VI,* P. I. Corke and J. Trevelyan (Eds.), Lecture Notes in Control and Information Sciences, Vol. 250, Springer-Verlag, pp. 403-412.

[7] James, D. L., Pai D. K. 2001. A Unified Treatment of Elastostatic and Rigid Contact Simulation for Real Time Haptics. *Haptics-e,* 2(1).

[8] Lozano, R., Brogliato, B., Egeland, O., Mashke, B. 2000. *Dissipative Systems, Analysis and Control, Theory and Applications.* Springer Verlag: New York.

[9] Mahvash, M., Hayward, V., Lloyd, J. E. 2002. Haptic Rendering of Tool Contact. Proc. *Eurohaptics 2002.* pp. 110–115.

[10] Mahvash, M., Hayward, V. 2001. Haptic Rendering of Cutting, A Fracture Mechanics Approach. *Haptics-e.* 2(3).

[11] Miller, B., Colgate, J. E., Freeman, R. A. 1999. Guaranteed Stability of Haptic Systems with Nonlinear Virtual Environments. *IEEE T. on Robot. Automat.*

[12] Niemeyer, G. , Slotine, J. J. 1991. Stable Adaptive Teleoperation. *IEEE J. Ocean. Eng.*, 16:152–162.

[13] Salisbury, K., Brock, D., Massie T., Swarup, N., Zilles, C. 1995. Haptic Rendering : Programming Touch Interaction with Virtual Objects. Proc. *Symposium on Interactive 3D Graphics,* ACM. pp. 123–130.

[14] Y. Yokokohji, Y., Imaida, T., Yoshikawa, T. 2000. Bilateral Control with Energy Balance Monitoring Under Time-varying Communication Delay, Proc. *IEEE Int. Conf. Robot. Automat.* pp. 2684–2689.

[15] Zilles, C. B., Salisbury, J. K. 1995. A Constraint-based God Object Method for Haptic Display. Proc. *IEEE Int. Conf. Intel. Rob. and Syst.,* Vol. 3, pp. 146–151.